



OPEN

MHD micropolar hybrid nanofluid flow over a flat surface subject to mixed convection and thermal radiation

Showkat Ahmad Lone¹, Maryam Ahmed Alyami², Anwar Saeed³, Abdullah Dawar⁴, Poom Kumam^{3,5}✉ & Wiyada Kumam⁶✉

Hybrid nanofluids play a significant role in the advancement of thermal characteristics of pure fluids both at experimental and industrial levels. This work explores the mixed convective MHD micropolar hybrid nanofluid flow past a flat surface. The hybrid nanofluid flow is composed of alumina and silver nanoparticles whereas water is used as a base fluid. The plate has placed vertical in a permeable medium with suction and injection effects. Furthermore, viscous dissipation, thermal radiation and Joule heating effects are taken into consideration. Specific similarity variables have been used to convert the set of modeled equations to dimension-free form and then has solved by homotopy analysis method (HAM). It has revealed in this investigation that, fluid motion upsurge with growth in magnetic field effects and mixed convection parameter and decline with higher values of micropolar factor. Micro-rotational velocity of fluid is upsurge with higher values of micropolar factor. Thermal flow behavior is augmenting for expended values of magnetic effects, radiation factor, Eckert number and strength of heat source. The intensification in magnetic strength and mixed convection factors has declined the skin friction and has upsurge with higher values of micropolar parameter. The Nusselt number has increased with the intensification in magnetic effects, radiation factor and Eckert number.

The fluid flow across a fixed surface is an important topic of fluid mechanics, which was first introduced by Blasius¹. Later on, Sakiadis² modified this problem to the fluid flow over a moving surface. Such types of flow problems have received much attention of researchers, due to their tremendous applications in engineering and industries, such as plastic extrusion, continuous casting, glass fiber and crystal development³. The Blasius and Sakiadis idea were further explained by the number of researchers, using different type of physical impacts and techniques⁴⁻⁸. Ishak et al.⁹ documented the flow and energy propagation characteristics of an incompressible nanofluid flow across a fixed and moving plane sheets. It was perceived that the energy transport rate boosts with the inclusion of nano particulates in the base fluid. Nadeem and Hussain¹⁰ reported the energy transmission through non-Newtonian Williamson nanoliquid flow over a heat fixed surface.

The fluid that comprising of micro-scale elements and possessing internal micro-structure characteristics is termed as micropolar fluid. These fluids exhibit micro-rotational inertial characteristics and micro-rotational phenomena. Micropolar fluid has several uses inside the electronic circuits, textiles, plastic sheet, power generations turbine and other excessive heated parts of heavy machinery¹¹. Many studies have been published with focal emphasis upon heat transfer characteristics by employing micropolar fluid. Magyari et al.¹² have used micropolar fluid flow with thermal flow through permeable stretched surface. Modather et al.¹³ provided a mathematical solution to the issue of energy and mass transmission of an oscillating two-dimensional electrically conducting

¹Department of Basic Sciences, College of Science and Theoretical Studies, Saudi Electronic University, (Jeddah-M), Riyadh 11673, Saudi Arabia. ²Department of Mathematics, Faculty of Sciences, University of Jeddah, Jeddah, Saudi Arabia. ³Center of Excellence in Theoretical and Computational Science (TaCS-CoE), Science Laboratory Building, Faculty of Science, King Mongkut's University of Technology Thonburi (KMUTT), 126 Pracha-Uthit Road, Bang Mod, Thung Khru, Bangkok 10140, Thailand. ⁴Department of Mathematics, Abdul Wali Khan University, Mardan 23200, Khyber Pakhtunkhwa, Pakistan. ⁵Department of Medical Research, China Medical University Hospital, China Medical University, Taichung 40402, Taiwan. ⁶Applied Mathematics for Science and Engineering Research Unit (AMSERU), Program in Applied Statistics, Department of Mathematics and Computer Science, Faculty of Science and Technology, Rajamangala University of Technology Thanyaburi (RMUTT), Pathum Thani 12110, Thailand. ✉email: poom.kum@kmutt.ac.th; wiyada.kum@rmutt.ac.th

micropolar fluid across an infinitely moving porous surface. Li et al.¹⁴ scrutinized heat transfer for micropolar hybrid nanofluid flow over an extending sheet and have exposed that augmentation in micropolar parameter and concentration of nanoparticles have upsurge the micropolar function. Bilal et al.¹⁵ discussed the influence of activation energy overheat transfer for micropolar fluid by using different properties and have highlighted that fluid flow speed has weakened with expansion in viscosity parameter, whereas thermal profiles have retarded with higher values of thermal conductivity factor. Krishna et al.¹⁶ have observed micropolar fluid flow with Darcy–Forchheimer model amid two rotary plates and have deduced that motion of fluid has weakened with expanding values of inertial factor.

The suspension of a single kind of small sized particle in a pure fluid for improvement of its thermal conductance is characterized as nanofluid. It has demonstrated experimentally that; such fluids have higher thermal conductivity. The small sized particles are known as nanoparticles. The idea of suspending nanoparticles into pure fluid was floated first by Choi and Eastman¹⁷ for improvement of the thermal conductivity of base fluid. An innovative category of fluid called hybrid nanofluid is helpful for the transition of energy. Numerous thermal applications, including freezing, renewable power, hvac systems, warm air converters, air conditioning units, transceivers, motorized industry, rechargeable cooler, ionizing radiation systems, vessels, and bioengineering, can make use of hybrid nanofluids. Bhatti et al.¹⁸ have inspected the MHD nano-liquid flow amid two rotary surfaces with influence of microorganism inside the plates and revealed that fluid flow has declined, and thermal characteristics have enhanced with growth in volumetric fraction. Shah et al.¹⁹ forwarded the idea of Srinivas et al.²⁰ by taking the impact of micropolar nanofluid flow with gold nanoparticles inside two plates and revealed that higher values of magnetic parameter has retarded the linear motion of fluid but has upsurge the micro-rotational motion. With the passage of time, it has noticed by the researchers and scientists that hanging of two distinct kinds of nanoparticles into pure fluid has augmented the thermal conductivity of pure fluids to better level. It has further established in various investigations^{21–27}, that thermal flow performance of hybrid nanofluid is much better than traditional nanofluids. Bilal et al.²⁸ analyzed the influence of variations in thermal conductance and heat generation for MHD hybrid nanomaterial through a permeable medium by employing slip condition and have concluded that with upsurge in nanoparticles concentration the Nusselt number has enlarged for shrinking case and has declined for stretching case. Salahiddin et al.²⁹ have examined the features of hybrid nanofluid in the closed vicinity of a highly magnetized cylinder. Alharbi et al.³⁰ has investigated numerically the effects of hybrid nanofluid upon an extending plate.

In the Joule heating phenomenon, electric energy is transformed to thermal energy because of resistive force to flow of current. The idea was first discovered by Joule³¹ in 1840. For its important applications in heat transfer phenomena, many investigations have been conducted keeping in mind the Joule heating effects. Loganathan and Rajan³² have inspected the irreversibility production for Williamson nanofluid flow subject to Joule heating influences with a conclusion that the thermal and mass flow rates is in inverse proportion of Weissenberg number. Nayak et al.³³ has analyzed fluid flow and heat transmission impact in a microchannel of hyperbolic form, packed with power law fluid subject to influence of Joule heating and have revealed that thermal flow rate of classical non-Newtonian and Newtonian fluids has augmented with upsurge in Joule heating factor and reduction in power index. Zhou et al.³⁴ examined the entropy production for MHD Newtonian fluid flow with influence of Joule heating and Darcy–Forchheimer model for flow system. Hafeez et al.³⁵ have discussed the influence of Joule heating upon Cattaneo–Christov double diffusion non-Newtonian fluid flow and have concluded that augmentation in solutal relaxation time and thermal factors have declined the profiles of concentration and temperature. Shamshuddin and Eid³⁶ have inspected effects of Joule heating upon mixed convective nanofluid flow over a stretched sheet and highlighted that Nusselt number has enlarged while fluid's velocity has weakened with growth in volumetric fraction.

Thermal radiation is one of several modes of thermal transmission and plays a substantial part in heat transfer and fluid flow problems. This term has achieved a remarkable progress in the field of thermal engineering and thermal sciences. Pramanik³⁷ has inspected thermal flow of fluid past an exponentially porous sheet using the influence of thermal radiations and has revealed that rate of thermal flow has enhanced for growth in thermal radiation and Casson factor. Khan et al.³⁸ have deliberated thermal and mass transmission for bioconvection nanofluid flow on Riga plate with influences of nonlinear thermal radiations. The authors of this work have established that concentration of fluid has enlarged with growth in thermophoretic and activation energy parameters whereas thermal flow profiles have been upsurge with various flow factors such as growth in thermophoresis, Brownian motion, magnetic and thermal radiation parameters. Ahmad et al.³⁹ have simulated the thermal radiations influence upon micropolar fluid flow in a permeable channel. Ibrahim et al.⁴⁰ have analyzed numerically two-dimensional unsteady fluid flow with thermally radiated effects upon flow system and concluded that temperature profiles have amplified with augmentation in radiation factor and Eckert number. Shaw et al.⁴¹ investigated MHD hybrid nanofluid flow subject to quadratic as well as nonlinear thermal radiations. Similar studies can be seen in Refs.^{42–46}.

Viscous dissipation performs as an energy source, modifying the temperature distribution and hence the heat transfer rate. Viscous dissipation is generated during deformation of fluid and connects the thermodynamics with dynamics. Waini et al.⁴⁷ has discussed micropolar hybrid nanofluid flow upon a stretching surface subject to viscous dissipation and thermophoresis effects and have explored that with upsurge in viscous dissipation parameter the thermal flow profiles have declined. Muntazir et al.⁴⁸ have scrutinized the MHD flow of fluid past a porous extending surface with impact of viscous dissipation and thermal radiations and have concluded that velocity, thermal as well as concentration characteristics have weakened with expansion in the values of time dependent and suction/injection parameters. Algehyne et al.⁴⁹ have deliberated the influence of viscous dissipation and nonlinear thermal radiations upon micropolar MHD fluid flow and have established that fluid flow has decayed with growth in magnetic parameter while thermal characteristics have enlarged with upsurge in electric, magnetic, thermal ratio and radiation factors. Upreti et al.⁵⁰ have evaluated the influence of suction

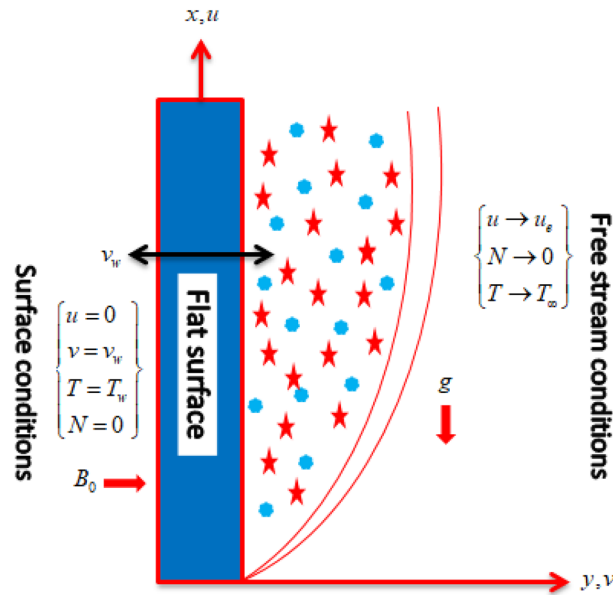


Figure 1. Flow geometry.

and viscous dissipation for Sisko fluid flow upon stretched sheet and have highlighted that in the occurrence of thermal source the thermal flow rate has enhanced with growth in Biot number. Yaseen et al.⁵¹ have deliberated hybrid nanofluid flow upon a thick concave/convex shaped subject to influences of Ohmic heating and viscous dissipation. Elattar et al.⁵² have analyzed numerically the thermal flow related to the influence of viscous dissipation and Joule heating. The readers can further study the similar concept in Refs.^{53–56}.

Being inspired by the above literature survey, the authors have verified that there is little work based on the micropolar hybrid nanofluid flow containing silver and alumina nanoparticles. The authors have considered the micropolar hybrid nanofluid flow containing silver and alumina nanoparticles past a stagnation point of a flat surface. The surface is placed vertical in a permeable medium with suction and injection effects. The mixed convection phenomenon is also taken into consideration. Furthermore, the viscous dissipation, thermal radiation and Joule heating impacts are taken into consideration. The present investigation is composed of problem formulation, which is shown in section “Problem formulation”, method of solution is presented in section “HAM solution”, results and discussion is presented in section “Results and discussion”, and the concluding remarks are displayed in section “Conclusion”.

Problem formulation

Consider the mixed convective MHD flow of a micropolar hybrid nanofluid at a stagnation point of flat sheet. The alumina and silver nanoparticles are mixed with water. B_0 is taken as strength of magnetic effects in the normal direction to fluid flow as shown in Fig. 1. The ambient motion is $u_e(x) = cx$, where c as positive constants. At the surface of sheet, the temperature is taken as $T_w(x) = T_\infty + bx$, where T_∞ and b are the ambient temperature and concentration, respectively. Further assumptions are considered as:

- Micropolar fluid is considered at a stagnation point.
- Mixed convection effects with heat source are employed to the flow system.
- Suction/injection, viscous dissipation, thermal radiations and Joule heating effects are taken into consideration.

Equations that administered flow problem are given as^{57,58}:

$$\frac{\partial u}{\partial x} + \frac{\partial v}{\partial y} = 0, \tag{1}$$

$$u \frac{\partial u}{\partial x} + v \frac{\partial u}{\partial y} = u_e \frac{du_e}{dx} + \frac{1}{\rho_{hmf}} (\mu_{hmf} + K_1) \frac{\partial^2 u}{\partial y^2} + \frac{K_1}{\rho_{hmf}} \frac{\partial N}{\partial y} - \frac{\sigma_{hmf}}{\rho_{hmf}} B_0^2 (u - u_e) + \frac{g(\rho\beta)_{hmf}}{\rho_{hmf}} (T - T_\infty), \tag{2}$$

$$u \frac{\partial N}{\partial x} + v \frac{\partial N}{\partial y} = \frac{\gamma_{hmf}}{\rho_{hmf}} \frac{\partial^2 N}{\partial y^2} - \frac{K_1}{\rho_{hmf} j} \left(2N + \frac{\partial u}{\partial y} \right), \tag{3}$$

Material	Water	Ag	Al ₂ O ₃
ρ	997.1	10,500	3970
C_p	4179	235	765
k	0.613	429	40
β	21×10^{-5}	1.89×10^{-5}	8.5×10^{-6}
σ	0.05	6.30×10^7	1×10^{-10}
Pr	6.2	-	-

Table 1. Numerical values of thermophysical properties for water and nanoparticles⁵⁹.

$$u \frac{\partial T}{\partial x} + v \frac{\partial T}{\partial y} = \frac{k_{hnf}}{(\rho C_p)_{hnf}} \frac{\partial^2 T}{\partial y^2} - \frac{1}{(\rho C_p)_{hnf}} \frac{\partial q_r}{\partial y} + \frac{Q_0}{(\rho C_p)_{hnf}} (T - T_\infty) + \frac{\mu_{hnf}}{(\rho C_p)_{hnf}} \left(\frac{\partial u}{\partial y} \right)^2 + \frac{\sigma_{hnf}}{(\rho C_p)_{hnf}} B_0^2 u^2, \tag{4}$$

Subject to the following boundary conditions:

$$\left\{ \begin{array}{l} u = 0, \quad v = v_w, \quad T = T_w, \quad N = 0 \quad \text{at } y = 0, \\ u \rightarrow u_e, \quad N \rightarrow 0, \quad T \rightarrow T_\infty \quad \text{as } y \rightarrow \infty. \end{array} \right\} \tag{5}$$

In Eq. (4), q_r is expressed mathematically as:

$$q_r = - \left(\frac{4\sigma^*}{3k^*} \frac{\partial T^4}{\partial y} \right). \tag{6}$$

By using Taylor expansion, T^4 is reduced as,

$$T^4 \cong 4TT_\infty^3 - 3T_\infty^4. \tag{7}$$

Thus, Eq. (4) is reduced as:

$$u \frac{\partial T}{\partial x} + v \frac{\partial T}{\partial y} = \left(\frac{k_{hnf}}{(\rho C_p)_{hnf}} + \frac{1}{(\rho C_p)_{hnf}} \frac{16\sigma^* T_\infty^3}{3k^*} \right) \frac{\partial^2 T}{\partial y^2} + \frac{Q_0}{(\rho C_p)_{hnf}} (T - T_\infty) + \frac{\mu_{hnf}}{(\rho C_p)_{hnf}} \left(\frac{\partial u}{\partial y} \right)^2 + \frac{\sigma_{hnf}}{(\rho C_p)_{hnf}} B_0^2 u^2, \tag{8}$$

Thermophysical properties of nanofluid and hybrid nanofluid are expressed as follows with numerical values as given in Table 1.

$$\left\{ \begin{array}{l} \frac{\rho_{nf}}{\rho_f} = (1 - \vartheta_{p1}) + \frac{\rho_{p1} \vartheta_{p1}}{\rho_f}, \quad \frac{(\rho C_p)_{nf}}{(\rho C_p)_f} = (1 - \vartheta_{p1}) + \vartheta_{p1} \frac{(\rho C_p)_{p1}}{(\rho C_p)_f}, \quad \frac{(\rho \beta)_{nf}}{(\rho \beta)_f} = (1 - \vartheta_{p1}) + \vartheta_{p1} \frac{(\rho \beta)_{p1}}{(\rho \beta)_f}, \\ \frac{\mu_{nf}}{\mu_f} = \frac{1}{(1 - \vartheta_{p1})^{2.5}}, \quad \frac{\sigma_{nf}}{\sigma_f} = 1 + \frac{3 \left[\left(\frac{\sigma_{p1}}{\sigma_f} - 1 \right) \vartheta_{p1} \right]}{\left(\frac{\sigma_{p1}}{\sigma_f} + 2 \right) - \left(\frac{\sigma_{p1}}{\sigma_f} - 1 \right) \vartheta_{p1}}, \quad \frac{k_{nf}}{k_f} = 1 + \frac{3 \left[\left(\frac{k_{p1}}{k_f} - 1 \right) \vartheta_{p1} \right]}{\left(\frac{k_{p1}}{k_f} + 2 \right) - \left(\frac{k_{p1}}{k_f} - 1 \right) \vartheta_{p1}}. \end{array} \right. \tag{9}$$

$$\left\{ \begin{array}{l} \frac{k_{hnf}}{k_f} = \frac{k_{p1} \vartheta_{p1} + k_{p2} \vartheta_{p2}}{\vartheta_{p1} + \vartheta_{p2}} + 2k_f + 2(k_{p1} \vartheta_{p1} + k_{p2} \vartheta_{p2}) - 2(\vartheta_{p1} + \vartheta_{p2})k_f, \\ \frac{\mu_{hnf}}{\mu_f} = \frac{1}{(1 - \vartheta_{p1} - \vartheta_{p2})^{2.5}}, \quad \frac{\rho_{hnf}}{\rho_f} = (1 - \vartheta_{p2}) \left[(1 - \vartheta_{p2}) + \vartheta_{p1} \frac{\rho_{p1}}{\rho_f} \right] + \vartheta_{p2} \frac{\rho_{p2}}{\rho_f}, \\ \frac{(\rho \beta)_{hnf}}{(\rho \beta)_f} = (1 - \vartheta_{p2}) \left[(1 - \vartheta_{p2}) + \vartheta_{p1} \frac{(\rho \beta)_{p1}}{(\rho \beta)_f} \right] + \vartheta_{p2} \frac{(\rho \beta)_{p2}}{(\rho \beta)_f}, \\ \frac{(\rho C_p)_{hnf}}{(\rho C_p)_f} = (1 - \vartheta_{p2}) \left[(1 - \vartheta_{p1}) + \vartheta_{p1} \frac{(\rho C_p)_{p1}}{(\rho C_p)_f} \right] + \vartheta_{p2} \frac{(\rho C_p)_{p2}}{(\rho C_p)_f}, \\ \frac{\sigma_{hnf}}{\sigma_f} = 1 + \frac{3 \left(\frac{\sigma_{p1} \vartheta_{p1} + \sigma_{p2} \vartheta_{p2}}{\sigma_f} \right) - 3(\vartheta_{p1} + \vartheta_{p2})}{2 + \left\{ \frac{\sigma_{p1} \vartheta_{p1} + \sigma_{p2} \vartheta_{p2}}{(\vartheta_{p1} + \vartheta_{p2}) \sigma_f} \right\} - \left\{ \frac{\sigma_{p1} \vartheta_{p1} + \sigma_{p2} \vartheta_{p2}}{\sigma_f} - (\vartheta_{p1} + \vartheta_{p2}) \right\}}, \end{array} \right. \tag{10}$$

The similarity transformations are defined as:

$$u = cx f', \quad v = -\sqrt{c v_f} f, \quad \xi = \sqrt{\frac{c}{v_f}} y, \quad N = cx \sqrt{\frac{c}{v_f}} g, \quad \theta = \frac{T - T_\infty}{T_w - T_\infty}. \tag{11}$$

Using Eq. (11), the leading equations are transformed as:

$$\left(\frac{1 + \chi_1 K}{\chi_1}\right) f''' + \chi_2 (1 + ff' - f'^2) + Kg' - M\chi_3 (f' - 1) + \lambda\chi_4 \theta = 0, \tag{12}$$

$$\left(\frac{2 + \chi_1 K}{\chi_1}\right) g'' + \chi_2 (g'f - gf') - K(f'' + 2g) = 0, \tag{13}$$

$$(\chi_6 + Rd)\theta'' + \frac{Ec Pr}{\chi_1} f'^2 + \chi_3 Ec Pr Mf'' + Pr \chi \theta + Pr \chi_5 (f\theta' - \theta f'') = 0. \tag{14}$$

Subjected conditions are given as:

$$\left\{ \begin{aligned} f'(\xi) = 0, \quad f(\xi) = S, \quad g(\xi) = 0, \quad \theta(\xi) = 1 \quad \text{at } \xi = 0, \\ G(\xi) \rightarrow 0, \quad f'(\xi) \rightarrow 1, \quad \theta(\xi) \rightarrow 0 \quad \text{as } \xi \rightarrow \infty. \end{aligned} \right\} \tag{15}$$

In the above equations, $K = K_1/\mu_f$ is the micropolar parameter, $\lambda = Gr_x/Re_x^2$ is the mixed convection parameter, $Gr_x = g\beta_f(T_w - T_\infty)x^3/v_f^2$ is the Grashof number, $Re_x = \frac{u_e(x)x}{v_f}$ is the Reynolds number, $Ec = u_e^2(x)/(C_p)_f(T_w - T_\infty)$ is the Eckert number, $Rd = 16\sigma^* T_\infty^3/3k_f k^*$ is the thermal radiation factor, $\chi = Q_0/c(\rho C_p)_f$ is the heat source/sink factor, $S = -v_w/\sqrt{c v_f}$ is the suction/injection parameter, $Pr = (\mu C_p)_f/k_f$ is the Prandtl number and $M = \sigma_f B_0^2/\rho_f c$ is the magnetic factor. It is also to be noticed that $\chi_1 = \mu_{hmf}/\mu_f$, $\chi_2 = \rho_{hmf}/\rho_f$, $\chi_3 = \sigma_{hmf}/\sigma_f$, $\chi_4 = (\rho\beta)_{hmf}/(\rho\beta)_f$, $\chi_5 = (\rho C_p)_{hmf}/(\rho C_p)_f$ and $\chi_6 = k_{hmf}/k_f$.

Important quantities. The important quantities skin friction coefficient (C_{fx}) and local Nusselt number (Nu_x) are mathematically described as:

$$C_{fx} = \frac{1}{\rho_{hmf} u_e^2(x)} \left[(\mu_{hmf} + K_1) \frac{\partial u}{\partial y} + K_1 N \right]_{y=0}. \tag{16}$$

$$Nu_x = - \left[\frac{x}{k_f (T_w - T_\infty)} \left(k_{hmf} \frac{\partial T}{\partial y} + \frac{16\sigma^*}{3k^*} \frac{\partial T^4}{\partial y} \right) \right]_{y=0}. \tag{17}$$

Using Eq. (11), the above equations are reduced as:

$$C_f = \frac{1}{\chi_2} \left[\frac{1 + \chi_1 K}{\chi_1} \right] f''(0). \tag{18}$$

$$Nu = -[\chi_6 + Rd]\theta'(0). \tag{19}$$

where $C_f = C_{fx}\sqrt{Re_x}$ and $Nu = \frac{Nu_x}{\sqrt{Re_x}}$.

HAM solution

In the current investigation the modeled equations have been converted to dimension-free format. The resultant equations gave rise to highly nonlinear differential equations. The HAM⁶⁰ method has been used to solve that set resultant equations. This technique is used to evaluate the highly nonlinear differential equations of fluid flow system and other similar problems. It is a fast convergent technique and is free from selection of embedded parameter. This technique requires initial guesses and linear operators which are defined as:

$$\left\{ \begin{aligned} f_0(\xi) &= \xi - 1 + e^{-\xi}, \\ g_0(\xi) &= 0, \\ \theta_0(\xi) &= e^{-\xi}, \end{aligned} \right\} \tag{20}$$

$$\left\{ \begin{aligned} L_f(\xi) &= \frac{\partial^3 f}{\partial \xi^3} + \frac{\partial f}{\partial \xi}, \\ L_g(\xi) &= \frac{\partial^2 g}{\partial \xi^2} + g, \\ L_\theta(\xi) &= \frac{\partial^2 \theta}{\partial \xi^2} + \theta, \end{aligned} \right\} \tag{21}$$

with properties:

$$\begin{cases} L_f(\varepsilon_1 + \varepsilon_2 e^{-\xi} + \varepsilon_3 e^{\xi}) = 0, \\ g_0(\varepsilon_4 e^{-\xi} + \varepsilon_5 e^{\xi}) = 0, \\ \theta_0(\varepsilon_6 e^{-\xi} + \varepsilon_7 e^{\xi}) = 0, \end{cases} \quad (22)$$

where $\chi_1 - \chi_7$ are the constant of general solution.

Convergence analysis. In order to employ HAM, we need to determine the solutions for velocity, micro-rotational velocity and temperature in the form of series. For convergence of these solutions the auxiliary functions \tilde{h}_f , \tilde{h}_g , \tilde{h}_θ come across which play a pivotal role in the convergence of method. For the purpose of this convergence, we have evaluated \tilde{h} -curves at 12th order of approximations as depicted in Fig. 2a–c. Figure 2a shows the convergence of $f''(0)$. From here, we see that $f''(0)$ converges at $-0.4 \leq \tilde{h}_f \leq 0.3$. Figure 2b shows the convergence of $g'(0)$. From here, we see that $g'(0)$ converges at $-0.3 \leq \tilde{h}_g \leq 0.35$. Figure 2c shows the convergence of $\theta'(0)$. From here, we see that $\theta'(0)$ converges at $-0.3 \leq \tilde{h}_\theta \leq 0.35$.

Results and discussion

This study explores the MHD natural convective micropolar hybrid nanofluid flow past a stretching plate. The fluid has influenced by thermal radiations and Joule heating effects. The plate has placed vertical in a permeable medium with suction and injection effects. The parameters that have influenced the current investigation have been discussed in following paragraphs. Figure 1 describes the fluid flow problem. Figure 2 presents the convergence analysis of the solution method for current investigation. It is to be noticed that throughout the discussion of results with the help of graphical view, we have used fixed computational values for substantial factors such as $Pr = 6.2$, $Rd = 1$, $Q = Ec = K = 0.5$, $\lambda = 0.5$, $\phi_1 = \phi_2 = 0.04$. The influence of different substantial parameters upon velocity $f'(\xi)$ and micro-rotational velocity $g(\xi)$ profiles has depicted in Figs. 3, 4, 5, 6, 7, 8. In Figs. 3 and 4 the influence of micropolar parameter K upon $f'(\xi)$ and $g(\xi)$ has presented. Since with growing values of K extra resistive force is experienced by the fluid motion in the linear direction of motion while the rotational motion is supported in this process. Hence higher values of K weaken the values of $f'(\xi)$ and upsurge the values of $g(\xi)$ as depicted in Figs. 3 and 4 respectively. Figure 5 presents that augmenting values of magnetic factor M results in the upsurge of momentum boundary layer strength. Hence growth in magnetic effects augments the fluid velocity of flow system. In case of micro-rotational velocity there is two-fold behavior of M upon $g(\xi)$. In the interval $0 < \xi < 1$ there is a reduction in the values of $g(\xi)$ whereas in the domain $1 < \xi < 6$ the strength of momentum boundary layer augments that upsurges the micro-rotational velocity of fluid motion as illustrated in Fig. 6. For growth in mixed convection parameter λ the buoyancy forces augment, that supports the linear velocity of fluid flow system. Hence upsurge in λ results an augmentation in $f'(\xi)$ as depicted in Fig. 7. In the similar manner as for magnetic effects again there is a two-fold behavior of variations in λ against the values of $g(\xi)$. Clearly in the interval $0 < \xi < 1$ there is a reduction in the values of $g(\xi)$, while in the domain $1 < \xi < 6$ the thickness of momentum boundary layer augments that upsurges the micro-rotational velocity of fluid motion as depicted in Fig. 8. Impact of different substantial factors upon thermal flow profiles has been depicted in Figs. 9, 10, 11, 12, 13. Variations in thermal profiles subject to changes in radiation factor Rd are illustrated in Fig. 9. The numerical values of Rd present the input comparison of thermal transmission via conduction of transfer via thermal radiation; hence with augmentation in Rd maximum heat diffusion occurs. Therefore, with upsurge in the values of Rd thermal profiles augment as described in Fig. 9. Application of the effects of magnetic factor M to a fluid motion produces Lorentz force that strongly opposes the motion in reverse direction. Hence growth in M generates more skin friction that results an upsurge in the thermal profiles as illustrated in Fig. 10. The variations in thermal flow with respect to heat generation and absorption factor χ are depicted in Fig. 11. It is obvious that for positive values of χ a heat generation “that is source” is found in the fluid flow. Hence growth in χ results an augmentation in thermal flow profiles as presented in Fig. 11. The influence of micro-polar factor K upon thermal profiles has depicted in Fig. 12. Since with growth in K the heating effects augment within the layer of thermal boundary region, hence higher values of K upsurge the values of thermal profiles. Figure 13 depicts variations in thermal profiles in response of changes in Eckert number Ec . Actually, Ec is employed to establish the effects of self-heating of fluid flow due to influence of dissipation. Hence, due to growth in Ec the thermal characteristics of micropolar fluid upsurge. Figure 14 shows the streamlines pattern for different values of M . Here, it is noted that with the increasing M , the streamlines patterns also increase. In Table 1 the numerical calculations for thermophysical characteristics are illustrated. Table 2 shows the comparison $f''(0)$ with published results. Here, a great agreement is found with those published results. In Table 3 the impact of various substantial factors over skin friction of fluid flow system has been portrayed in numerical manners. Since the fluid motion has upsurge with expansion in magnetic effects and mixed convection factor while it has declined with augmenting values of micropolar factor. Hence intensification in magnetic strength and mixed convection factors has declined the skin friction and has upsurge with higher values of micropolar parameter. Actually, with upsurge in magnetic strength and mixed convection, lesser friction has experienced by the micropolar nanoparticles at the surface of stretching sheet that has declined skin friction in the closed locality of stretching plate. The numerical impacts of different substantial factors upon fluid's thermal flow rate have been depicted in Table 4. Since for growth in magnetic effects, radiation factor and Eckert number and in strength of heat source the thermal flow of micropolar fluid augment, hence the Nusselt number has increased with intensification in the values of these parameters.

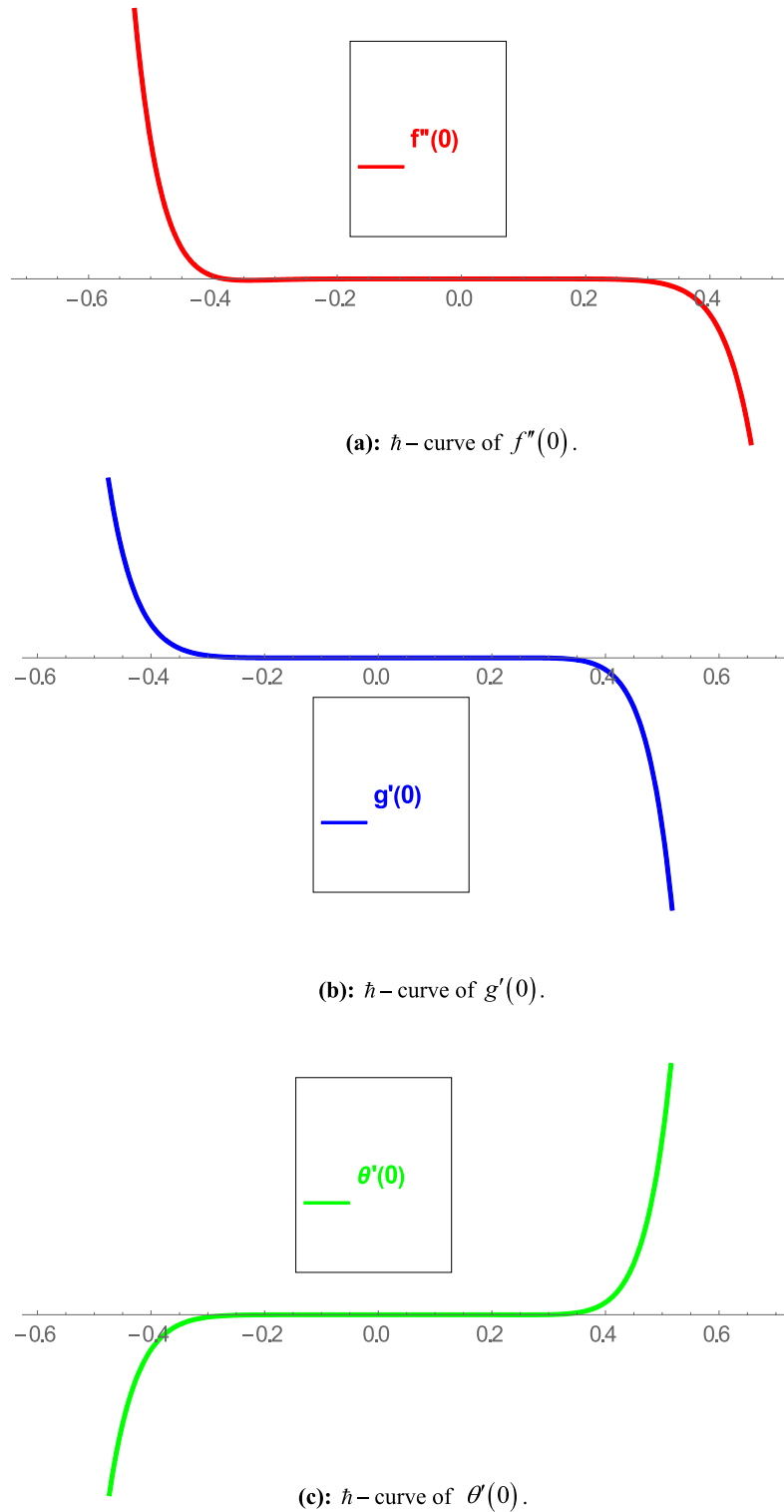


Figure 2. (a) h -curve of $f''(0)$. (b) h -curve of $g'(0)$. (c) h -curve of $\theta'(0)$.

Conclusion

This study explores mixed convective MHD micropolar water-based hybrid nanofluid flow containing silver and alumina past a flat surface. The hybrid nanofluid flow is taken under viscous dissipation, thermal radiation and Joule heating effects. The surface is placed vertical in a permeable medium with suction and injection effects. Specific similarity variables have used to transform the set of modeled equations to dimension-free form and then solved by HAM. Following main points have been concluded:

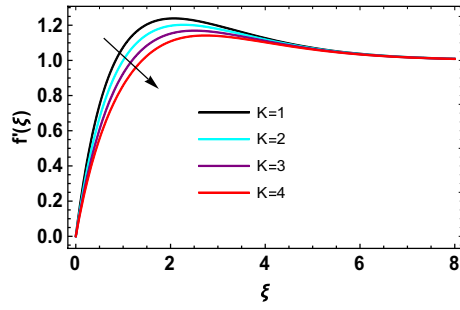


Figure 3. Impact of K upon $f'(\xi)$.

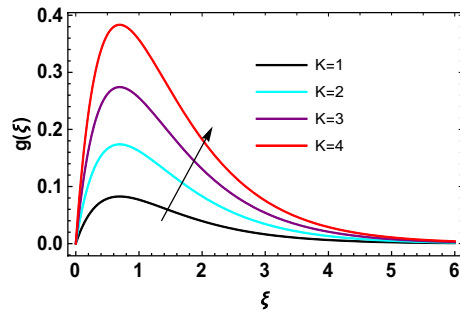


Figure 4. Impact of K upon $g(\xi)$.

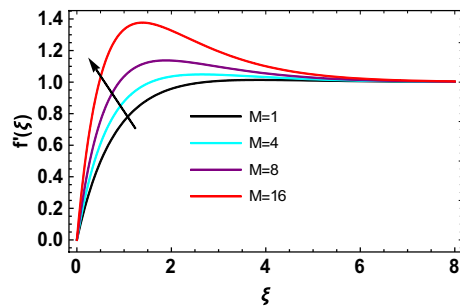


Figure 5. Impact of M upon $f'(\xi)$.

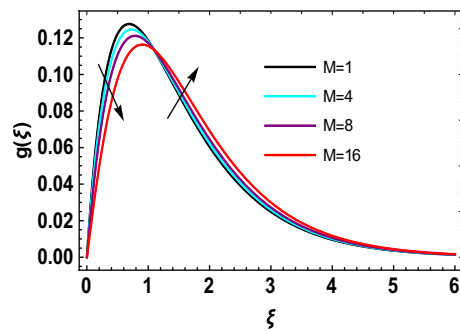


Figure 6. Impact of M upon $g(\xi)$.

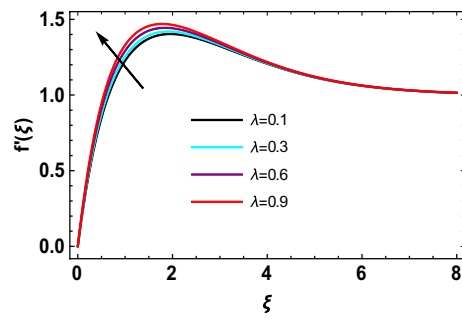


Figure 7. Impact of λ upon $f'(\xi)$.

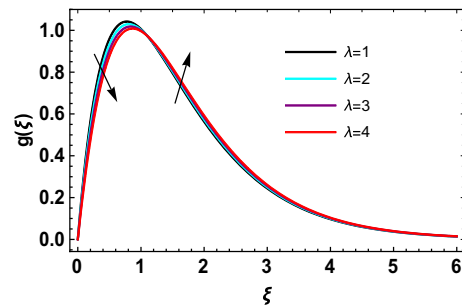


Figure 8. Impact of λ upon $g(\xi)$.

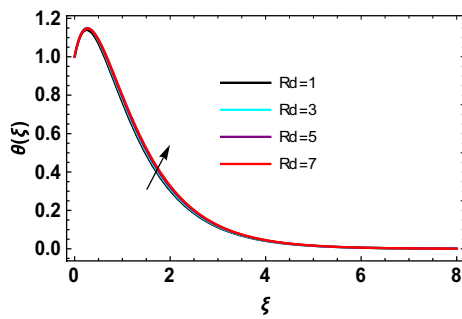


Figure 9. Impact of Rd on $\theta(\xi)$.

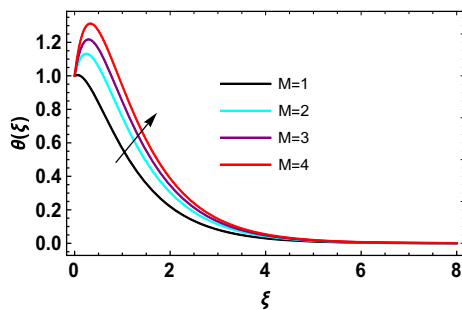


Figure 10. Impact of M on $\theta(\xi)$.

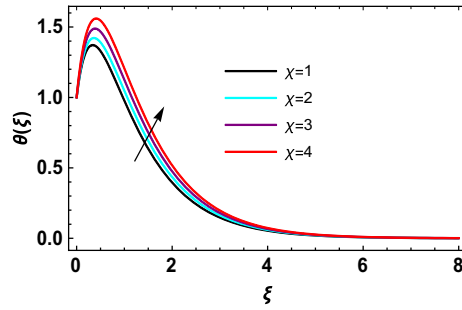


Figure 11. Impact of χ on $\theta(\xi)$.

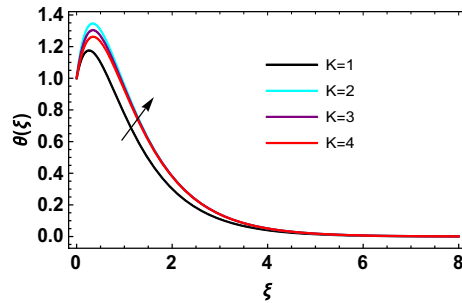


Figure 12. Impact of K on $\theta(\xi)$.

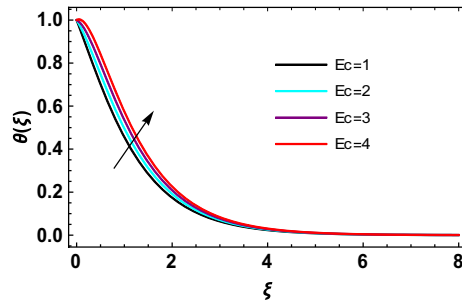


Figure 13. Impact of Ec on $\theta(\xi)$.

1. Fluid motion upsurges with the increase in magnetic parameter and mixed convection parameter while reduces with the growth in micropolar factor.
2. Micro-rotational velocity of fluid upsurges with higher values of micropolar factor.
3. For growth in mixed convection and magnetic factors the micro-rotational motion exhibits two-fold behavior. In the interval $0 < \xi < 1$ there is a reduction while in the domain $1 < \xi < 6$ there is a growth in micro-rotational motion for higher values of both parameters.
4. Thermal flow behavior is augmenting for expanded values of magnetic effects, radiation factor, Eckert number and heat source strength.
5. The intensification in magnetic strength and mixed convection factors has declined the skin friction and has upsurge with higher values of micropolar parameter.
6. The Nusselt number has increased with the intensification in magnetic effects, radiation factor and Eckert number.

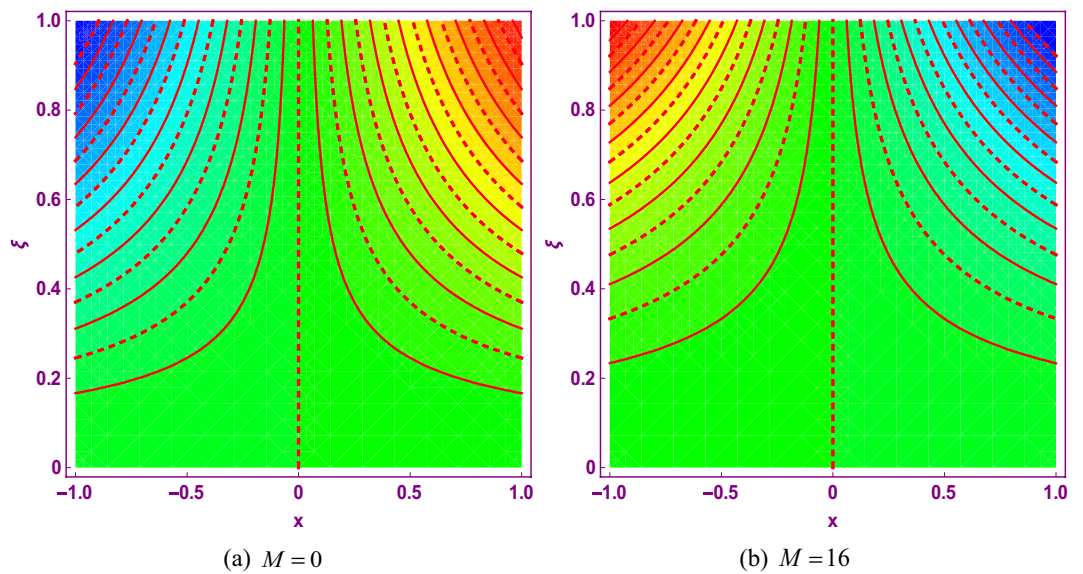


Figure 14. Streamlines patterns for $M = 0$ and $M = 16$.

Pr	Zaib et al. ⁶¹	Present results
0.7	1.7063	1.7063
1.0	1.6754	1.6754
7.0	1.5179	1.5179
10.0	1.4928	1.4928

Table 2. Comparison of $f''(0)$ with published results of Zaib et al.⁶¹, when $\lambda = 0$ and all other parameters are zero.

M	λ	K	C_f
0.5			-0.274370
1.0			-0.345012
1.5			-0.415654
2.0			-0.486296
	0.1		-0.246938
	0.2		-0.253796
	0.3		-0.260654
	0.4		-0.267512
		0.1	0.216446
		0.2	0.256543
		0.3	0.290717
		0.4	0.318968

Table 3. Influences of M, λ and K on C_f .

M	Rd	Ec	χ	Nu
0.5				0.290790
1.0				0.350868
1.5				0.410947
2.0				0.471025
	0.1			0.290790
	0.3			0.295220
	0.5			0.299650
	0.7			0.304079
		1.0		0.539396
		2.0		1.036606
		3.0		1.533817
		4.0		2.031028
			1.1	0.284866
			1.2	0.290790
			1.3	0.290790
			1.4	0.302638

Table 4. Influences of M , Rd , Ec and χ on Nu .

Data availability

The data related to this manuscript are within the manuscript.

Received: 25 August 2022; Accepted: 26 September 2022

Published online: 14 October 2022

References

- Blasius, H. *Grenzschichten in Flüssigkeiten mit kleiner Reibung* (Druck von BG Teubner, 1907).
- Sakiadis, B. C. Boundary-layer behavior on continuous solid surfaces: I. Boundary-layer equations for two-dimensional and axisymmetric flow. *AIChE J.* **7**, 26–28 (1961).
- Bachok, N., Ishak, A. & Pop, I. Boundary-layer flow of nanofluids over a moving surface in a flowing fluid. *Int. J. Therm. Sci.* **49**, 1663–1668 (2010).
- Bataller, R. C. Radiation effects in the Blasius flow. *Appl. Math. Comput.* **198**, 333–338 (2008).
- Aziz, A. A similarity solution for laminar thermal boundary layer over a flat plate with a convective surface boundary condition. *Commun. Nonlinear Sci. Numer. Simul.* **14**, 1064–1068 (2009).
- Ishak, A., Yacob, N. A. & Bachok, N. Radiation effects on the thermal boundary layer flow over a moving plate with convective boundary condition. *Meccanica* **46**, 795–801 (2011).
- Ramesh, G. K., Gireesha, B. J. & Gorla, R. S. R. Study on Sakiadis and Blasius flows of Williamson fluid with convective boundary condition. *Nonlinear Eng.* **4**, 215–221 (2015).
- Ishak, A., Nazar, R. & Pop, I. Flow and heat transfer characteristics on a moving flat plate in a parallel stream with constant surface heat flux. *Heat Mass Transf.* **45**, 563–567 (2009).
- Ishak, A., Nazar, R. & Pop, I. Boundary-layer flow of a micropolar fluid on a continuous moving or fixed surface. *Can. J. Phys.* **84**, 399–410 (2006).
- Nadeem, S. & Hussain, S. T. Analysis of MHD Williamson nano fluid flow over a heated surface. *J. Appl. Fluid Mech.* **9**, 729–739 (2016).
- Eringen, A. C. Theory of micropolar fluids. *J. Math. Mech.* **16**, 1–18. <http://www.jstor.org/stable/24901466> (1966).
- Magyari, E. & Chamkha, A. J. Combined effect of heat generation or absorption and first-order chemical reaction on micropolar fluid flows over a uniformly stretched permeable surface: The full analytical solution. *Int. J. Therm. Sci.* **49**, 1821–1828 (2010).
- Modather, M., Rashad, A. M. & Chamkha, A. J. An analytical study of MHD heat and mass transfer oscillatory flow of a micropolar fluid over a vertical permeable plate in a porous medium. *Turk. J. Eng. Environ. Sci.* **33**, 245–258 (2009).
- Li, P. *et al.* Heat transfer of hybrid nanomaterials base Maxwell micropolar fluid flow over an exponentially stretching surface. *Nanomaterials* **12**, 1207 (2022).
- Bilal, M. *et al.* Parametric simulation of micropolar fluid with thermal radiation across a porous stretching surface. *Sci. Rep.* **12**, 1–11 (2022).
- Krishna, M. V., Ahamad, N. A. & Chamkha, A. J. Hall and ion slip effects on unsteady MHD free convective rotating flow through a saturated porous medium over an exponential accelerated plate. *Alex. Eng. J.* **59**, 565–577 (2020).
- Choi, S. U. S. & Eastman, J. A. Enhancing thermal conductivity of fluids with nanoparticles. *1995 Int. Mech. Eng. Congr. Exhib. San Fr. CA (United States)*, 12–17 Nov 1995 (1995). <https://digital.library.unt.edu/ark:/67531/metadc671104/> (Accessed October 2, 2021).
- Bhatti, M. M., Arain, M. B., Zeeshan, A., Ellahi, R. & Doranehgard, M. H. Swimming of gyrotactic microorganism in MHD Williamson nanofluid flow between rotating circular plates embedded in porous medium: Application of thermal energy storage. *J. Energy Storage* **45**, 103511 (2022).
- Shah, Z. *et al.* Micropolar gold blood nanofluid flow and radiative heat transfer between permeable channels. *Comput. Methods Programs Biomed.* **186**, 105197 (2020).
- Srinivas, S., Vijayalakshmi, A. & Reddy, A. S. Flow and heat transfer of gold-blood nanofluid in a porous channel with moving/stationary walls. *J. Mech.* **33**, 395–404 (2017).
- Sreedevi, P., Sudarsana Reddy, P. & Chamkha, A. Heat and mass transfer analysis of unsteady hybrid nanofluid flow over a stretching sheet with thermal radiation. *SN Appl. Sci.* **2**, 1–15 (2020).
- Krishna, M. V. & Chamkha, A. J. Hall and ion slip effects on MHD rotating boundary layer flow of nanofluid past an infinite vertical plate embedded in a porous medium. *Results Phys.* **15**, 102652 (2019).

23. Muthamilselvan, M., Suganya, S. & Al-Mdallal, Q. M. Stagnation-point flow of the Williamson nanofluid containing gyrotactic micro-organisms. *Proc. Natl. Acad. Sci. India Sect. A Phys. Sci.* **91**, 633–648 (2021).
24. Prakash, D., Ragupathi, E., Muthamilselvan, M., Abdalla, B. & AlMdallal, Q. M. Impact of boundary conditions of third kind on nanoliquid flow and radiative heat transfer through asymmetrical channel. *Case Stud. Therm. Eng.* **28**, 101488 (2021).
25. Sadham Hussain, I., Prakash, D., Kumar, S. & Muthamilselvan, M. Bioconvection of nanofluid flow in a thin moving needle in the presence of activation energy with surface temperature boundary conditions. *Proc. Inst. Mech. Eng. Part E J. Process Mech. Eng.* (2021).
26. Shafiq, A., Lone, S. A., Sindhu, T. N., Al-Mdallal, Q. M. & Rasool, G. Statistical modeling for bioconvective tangent hyperbolic nanofluid towards stretching surface with zero mass flux condition. *Sci. Rep.* **11**, 1–11 (2021).
27. Khan, M., Lone, S. A., Rasheed, A. & Alam, M. N. Computational simulation of Scott–Blair model to fractional hybrid nanofluid with Darcy medium. *Int. Commun. Heat Mass Transf.* **130**, 105784 (2022).
28. Bilal, M. *et al.* Numerical analysis of an unsteady, electroviscous, ternary hybrid nanofluid flow with chemical reaction and activation energy across parallel plates. *Micromachines* **13**, 874 (2022).
29. Salahuddin, T., Siddique, N., Khan, M. & Chu, Y. A hybrid nanofluid flow near a highly magnetized heated wavy cylinder. *Alex. Eng. J.* **61**, 1297–1308 (2022).
30. Alharbi, K. A. M. *et al.* Computational valuation of Darcy ternary-hybrid nanofluid flow across an extending cylinder with induction effects. *Micromachines* **13**, 588 (2022).
31. Joule, J. P. On the production of heat by voltaic electricity. In *Abstr. Pap. Print. Philos. Trans. R. Soc. London* 280–282 (The Royal Society London, 1843).
32. Loganathan, K. & Rajan, S. An entropy approach of Williamson nanofluid flow with Joule heating and zero nanoparticle mass flux. *J. Therm. Anal. Calorim.* **141**, 2599–2612 (2020).
33. Zhou, S.-S., Bilal, M., Khan, M. A. & Muhammad, T. Numerical analysis of thermal radiative Maxwell nanofluid flow over-stretching porous rotating disk. *Micromachines* **12**, 540 (2021).
34. Khan, S. A. *et al.* Irreversibility analysis in hydromagnetic flow of Newtonian fluid with Joule heating: Darcy–Forchheimer model. *J. Pet. Sci. Eng.* **212**, 110206 (2022).
35. Hafeez, A., Khan, M., Ahmed, A. & Ahmed, J. Features of Cattaneo–Christov double diffusion theory on the flow of non-Newtonian Oldroyd-B nanofluid with Joule heating. *Appl. Nanosci.* **12**, 265–272 (2022).
36. Shamshuddin, M. D. & Eid, M. R. nth order reactive nanoliquid through convective elongated sheet under mixed convection flow with joule heating effects. *J. Therm. Anal. Calorim.* **147**, 3853–3867 (2022).
37. Pramanik, S. Casson fluid flow and heat transfer past an exponentially porous stretching surface in presence of thermal radiation. *Ain Shams Eng. J.* **5**, 205–212 (2014).
38. Khan, M. I., Shah, F., Khan, S. U., Ghaffari, A. & Chu, Y. Heat and mass transfer analysis for bioconvective flow of Eyring Powell nanofluid over a Riga surface with nonlinear thermal features. *Numer. Methods Partial Differ. Equ.* **38**, 777–793 (2022).
39. Ahmad, S., Ashraf, M. & Ali, K. Simulation of thermal radiation in a micropolar fluid flow through a porous medium between channel walls. *J. Therm. Anal. Calorim.* **144**, 941–953 (2021).
40. Ibrahim, M., Saeed, T. & Zeb, S. Numerical simulation of time-dependent two-dimensional viscous fluid flow with thermal radiation. *Eur. Phys. J. Plus* **137**, 609 (2022).
41. Shaw, S., Samantaray, S. & Misra, A. *Hydromagnetic Flow and Thermal Interpretations of Cross Hybrid Nanofluid Influenced by Linear, Nonlinear and Quadratic Thermal Radiations for any Prandtl Number* (Elsevier, 2022).
42. VeeraKrishna, M., Subba Reddy, G. & Chamkha, A. J. Hall effects on unsteady MHD oscillatory free convective flow of second grade fluid through porous medium between two vertical plates. *Phys. Fluids*. **30**, 23106 (2018).
43. Krishna, M. V. & Chamkha, A. J. Hall and ion slip effects on MHD rotating flow of elasto-viscous fluid through porous medium. *Int. Commun. Heat Mass Transf.* **113**, 104494 (2020).
44. Krishna, M. V., Ahamad, N. A. & Chamkha, A. J. Hall and ion slip impacts on unsteady MHD convective rotating flow of heat generating/absorbing second grade fluid. *Alex. Eng. J.* **60**, 845–858 (2021).
45. Chamkha, A. J. Solar radiation assisted natural convection in uniform porous medium supported by a vertical flat plate (1997).
46. Sandeep, N., Chamkha, A. J. & Animasaun, I. L. Numerical exploration of magnetohydrodynamic nanofluid flow suspended with magnetite nanoparticles. *J. Braz. Soc. Mech. Sci. Eng.* **39**, 3635–3644. <https://doi.org/10.1007/S40430-017-0866-X> (2017).
47. Waini, I., Khan, U., Zaib, A., Ishak, A., Pop, I. Thermophoresis particle deposition of CoFe₂O₄-TiO₂ hybrid nanoparticles on micropolar flow through a moving flat plate with viscous dissipation effects. *Int. J. Numer. Methods Heat Fluid Flow* (2022).
48. Muntazir, R. M. A., Mushtaq, M., Shahzadi, S., Jabeen, K. MHD nanofluid flow around a permeable stretching sheet with thermal radiation and viscous dissipation. *Proc. Inst. Mech. Eng. Part C J. Mech. Eng. Sci.* (2021).
49. Algehyne, E. A., Alriheli, H. F., Bilal, M., Saeed, A. & Weera, W. Numerical approach toward ternary hybrid nanofluid flow using variable diffusion and non-Fourier's concept. *ACS Omega* (2022).
50. Upreti, H., Joshi, N., Pandey, A. K. & Rawat, S. K. Assessment of convective heat transfer in Sisko fluid flow via stretching surface due to viscous dissipation and suction. *Nanosci. Technol. Int. J.* **13** (2022).
51. Yaseen, M., Rawat, S. K. & Kumar, M. Hybrid nanofluid (MoS₂-SiO₂/water) flow with viscous dissipation and Ohmic heating on an irregular variably thick convex/concave-shaped sheet in a porous medium. *Heat Transf.* **51**, 789–817 (2022).
52. Elattar, S. *et al.* Computational assessment of hybrid nanofluid flow with the influence of hall current and chemical reaction over a slender stretching surface. *Alex. Eng. J.* **61**, 10319–10331 (2022).
53. Takhar, H. S., Chamkha, A. J. & Nath, G. MHD flow over a moving plate in a rotating fluid with magnetic field, Hall currents and free stream velocity. *Int. J. Eng. Sci.* **40**, 1511–1527 (2002).
54. Chamkha, A. J. & Ben-Nakhi, A. MHD mixed convection–radiation interaction along a permeable surface immersed in a porous medium in the presence of Soret and Dufour's effects. *Heat Mass Transf.* **44**, 845–856 (2008).
55. Arafa, A. A. M., Ahmed, S. E. & Allan, M. M. Peristaltic flow of non-homogeneous nanofluids through variable porosity and heat generating porous media with viscous dissipation: Entropy analyses. *Case Stud. Therm. Eng.* **32**, 101882 (2022).
56. Mburu, Z. M., Nayak, M. K., Mondal, S. & Sibanda, P. Impact of irreversibility ratio and entropy generation on three-dimensional Oldroyd-B fluid flow with relaxation–retardation viscous dissipation. *Indian J. Phys.* **96**, 151–167 (2022).
57. Koriko, O. K., Oreyeni, T., Omowaye, A. J. & Animasaun, I. L. Homotopy analysis of MHD free convective micropolar fluid flow along a vertical surface embedded in non-Darcian thermally-stratified medium. *Open J. Fluid Dyn.* **6**, 198–221 (2016).
58. Hosseinzadeh, K., Roghani, S., Asadi, A., Mogharrebi, A. & Ganji, D. D. Investigation of micropolar hybrid ferrofluid flow over a vertical plate by considering various base fluid and nanoparticle shape factor. *Int. J. Numer. Methods Heat Fluid Flow* **31**, 402–417 (2020).
59. Job, V. M., Gunakala, S. R. & Chamkha, A. J. Numerical investigation of unsteady MHD mixed convective flow of hybrid nanofluid in a corrugated trapezoidal cavity with internal rotating heat-generating solid cylinder. *Eur. Phys. J. Spec. Top.*, 1–8 (2022).
60. Liao, S.-J. An explicit, totally analytic approximate solution for Blasius' viscous flow problems. *Int. J. Non Linear. Mech.* **34**, 759–778 (1999).
61. Zaib, A., Khan, U., Shah, Z., Kumam, P. & Thounthong, P. Optimization of entropy generation in flow of micropolar mixed convective magnetite (Fe₃O₄) ferroparticle over a vertical plate. *Alex. Eng. J.* **58**, 1461–1470 (2019).

Acknowledgements

The authors acknowledge the financial support provided by Thailand Science Research and Innovation (TSRI) and Rajamangala University of Technology Thanyaburi (RMUTT) under National Science, Research and Innovation Fund (NSRF); Basic Research Fund: Fiscal year 2022 (Contract No. FRB650070/0168 and under project number FRB65E0633M.2).

Author contributions

All authors equally contributed.

Competing interests

The authors declare no competing interests.

Additional information

Correspondence and requests for materials should be addressed to P.K. or W.K.

Reprints and permissions information is available at www.nature.com/reprints.

Publisher's note Springer Nature remains neutral with regard to jurisdictional claims in published maps and institutional affiliations.



Open Access This article is licensed under a Creative Commons Attribution 4.0 International License, which permits use, sharing, adaptation, distribution and reproduction in any medium or format, as long as you give appropriate credit to the original author(s) and the source, provide a link to the Creative Commons licence, and indicate if changes were made. The images or other third party material in this article are included in the article's Creative Commons licence, unless indicated otherwise in a credit line to the material. If material is not included in the article's Creative Commons licence and your intended use is not permitted by statutory regulation or exceeds the permitted use, you will need to obtain permission directly from the copyright holder. To view a copy of this licence, visit <http://creativecommons.org/licenses/by/4.0/>.

© The Author(s) 2022